www.czasopisma.pan.pl PAN www.journals.pan.pl
POLSKA AKADEMIA NAUK

Opto-Electronics Review 27 (2019) 25–31

Contents lists available at ScienceDirect

Opto-Electronics Review

journal homepage: http://www.journals.elsevier.com/opto-electronics review

# Control of simultaneous effects of the temperature, indium composition and the impact ionization process on the performance of the $InN/In_xGa_{1-x}N$ quantum dot solar cells

N. Ben Afkir[a,*], E. Feddi[b], J. Meziane[a], Y. EL Kouari[a], M. Zazoui[a], A. Migalska-Zalas[c,*]

[a] Laboratory of Condensed Matter and Renewable Energy, Faculty of Sciences and Technology, University Hassan II of Casablanca, BP146, Casablanca, Morocco
[b] Laboratoire de Matière Condensée et Sciences Interdisciplinaires (LaMCScI), Group of Optoelectronic of Semiconductors and Nanomaterials, ENSET, Mohammed V University in Rabat, Morocco
[c] Faculty of Mathematics and Natural Sciences, Institute of Physics, J. Dlugosz University of Czestochowa, Al. Armii Krajowej 13/15, Czestochowa, Poland

ARTICLE INFO

*Article history:*
Received 1 November 2018
Accepted 7 January 2019
Available online 11 February 2019

*Keywords:*
Impact ionization
*InGaN*
IBSC
Quantum dot
Solar cells
Energy

ABSTRACT

The impact ionization in semiconductor materials is a process that produces multiple charge carrier pairs from a single excitation. This mechanism constitutes a possible road to increase the efficiency of the *p-n* and *p-i-n* solar cells junctions. Our study considers the structure of *InN/InGaN* quantum dot solar cell in the calculation. In this work, we study the effect of indium concentration and temperature on the coefficient $\theta$ of the material type parameter of the impact ionization process for a *p(InGaN)-n(InGaN)* and *p(InGaN)-i(QDs-InN)-n(InGaN)* solar cell. Next, we investigate the effect of perturbation such as temperature and indium composition on conventional solar cell's *(p(InGaN)-n(InGaN))* and solar cells of the third generation with quantum dot intermediate band IBSC *(p(InGaN-i(QD-InN)-n(InGaN))* by analyzing their behaviour in terms of efficiency of energy conversion at the presence of the impact ionization process. Our numerical results show that the efficiency is strongly influenced by all of these parameters. It is also demonstrated that $\theta$ decreased with the increase of indium concentration and temperature which contributes to an overall improvement of the conversion efficiency.


## 1. Introduction

Photovoltaic conversion is extensively studied in the last years due to its potential to address the continuing decline of fossil resources [1–4]. Recently, many scientists suggested different patterns to increase the conversion efficiency of these devices. Among these models, the intermediate band solar cells (IBSC) were proposed by A. Luque in 1997 to provide higher efficiency and to exceed the Shockley–Queisser limit for a single-junction solar cell [5–7]. The principle of the IBSC consists of inserting an intermediate band based on multilayer quantum dots (QDs) between the p and n junctions [6]. Indeed, quantification of energy levels in quantum dots can create intermediate levels. On the other side, the solar cells based on the QD exhibit an electron–hole pair multiplication, which leads to provide higher efficiency limit [8,9]. A QDs-IBSC cell can be manufactured, for example, by using a molecular beam epitaxial in Stranski-Krastanov growth mode composed of the lower layers of QDs sandwiched by p and n *GaAs* transmitters [10]. Thus, the uses of the QDs in the solar cells have been shown to have an interesting potential to reduce energy loss corresponding to the photons with low energy [11–13]. On the other hand the thermalization effect is among factors limiting the efficiency limit. In order to recuperate the energy lost by thermalization, some studies have used the impact ionization process into a single-junction solar cell [14–17]. This process requires incident photon energy greater than the $\theta E_g$, where $\theta$ is coefficient of the selected material of impact ionization process. We note that transitions related to the impact ionization result from the collision between an electron of the conduction band and another electron of the valence band. So, the electron in the conduction band loses its energy and moves therefore to a lower energetic band in the same conduction band. However, another electron of the valence band recovers the energy lost during the collision to get promoted to the conduction band. The mechanisms applying to bulk materials, as well as to those based on QDs are respectively presented in Figs. 1(a) and 1(b) [1].

Different previous works have generally studied only the variation in efficiency as a function of the coefficient of the material

* Corresponding authors.
*E-mail addresses:* ben.afkir.noureddine@gmail.com (N. Ben Afkir), aniazal@op.pl (A. Migalska-Zalas).

https://doi.org/10.1016/j.opelre.2019.01.004

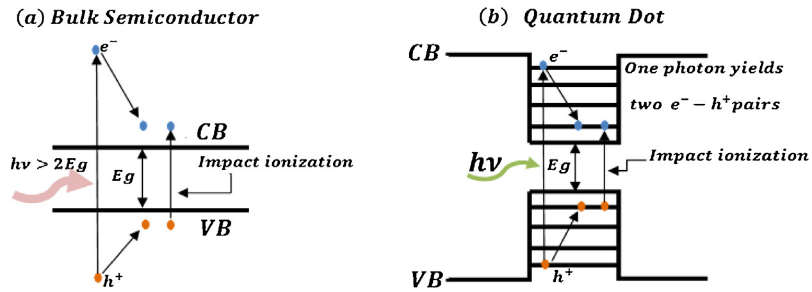


**Fig. 1.** The different steps of creating electron-hole pairs by impact ionization process in the case of a bulk semiconductor [1(a)] and in the case of a QD [1(b)] taken from [1].

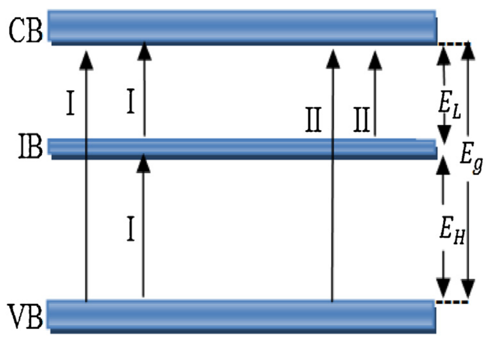


**Fig. 2.** Energy bands in *p-i-n* junction solar cells with intermediate band based on QDs.

type parameter and ionization impact probability [14,17,18], but it is also interesting to study the effect of other parameters such as temperature and *In* concentration. It is expected that by controlling the above mentioned parameters and improving the properties of the materials used in the cell, it is possible to exceed the S-Q limit. In the following, we present the impact of the different parameters on the efficiency of solar cells based on *InGaN* material. Let us underline that temperature or substitution degree, electronic and optical properties of semiconductor materials are considerably altered [19–22]. This results in a change of the impact-ionization process and of the energy conversion efficiency of both conventional solar cells *(p-n)* and intermediate band solar cells (QD-IBSC) *p-i-n* undergo a considerable change. In this field, we report an investigation of the *p(InGaN)-n(InGaN)* and *p(InGaN)-i(QD-InN)-n(InGaN)* junction solar cells. Calculation is discussed in the context of the effective mass approximation. In order to calculate energy levels of an intermediate band the Schrödinger equation in 3D is solved by using the finite difference method. We analyze the impact of temperature and indium concentration on the parameter that depends on the type of the selected material for impact ionization process. So, we take into account impact ionization process, effect of the temperature and indium content on energy conversion efficiency of conventional solar cells *(p-n)*, and intermediate band solar cell *(p-i-n)* are investigated. The paper is organized as follows. In Section 2, we outline our theoretical approach for evaluating the efficiency of a *p-n* and *p-i-n* junction. In Section 3, we present our numerical results and discussions.

## 2. Theoretical part

In this section two cases are investigated. In the former, we study the p-n junction where only transitions from the valence band to the conduction band are possible. In the latter, we are interested in the *p-i-n* junction where the additional transitions to and from the intermediate band are possible, see Fig. 2. In the second case, we distinguish between “direct” transitions, denoted I in Fig. 2, and the “other” transitions, denoted II. Both are triggered by the impact ionization mechanism which corresponds to the inverse of the Auger recombination process. In the first time we present the theoretical formulation for calculating electron, holes energy levels, interband $E_H$, and intersubband $E_L$ transition QD-IBSC. The system under investigation consists of spherical *InN* QDs embedded into a $In_xGa_{1-x}N$ matrix.

In spherical coordinate, the time-independent Schrödinger equation for electrons (holes) in conduction (valence) band into a spherical coordinate, in the effective mass approximation, is stated as follows [23]:

$$-\frac{\hbar^2}{2m_i^*}\left(\frac{2}{r_i}\frac{\partial}{\partial r_i}+\frac{\partial^2}{\partial {r_i}^2}\right)\psi(r_i)+\frac{\hbar^2 l(l+1)}{2m_i^* r_i^2}\psi(r_i)$$
$$+V_i(r_i)\psi(r_i)=E_i\psi(r_i) \quad (1)$$

where $r_i$ is the radial coordinate of the particle with $i=(e,h)$, $\psi(r_i)$ the radial wave function and $m_i^*$ is the effective mass depending on temperature and indium content $x$ in the structure [24]:

$$m_i^*(x,T)=\begin{cases} m^*_{i,InN}(T)\; r_i\le R\; in\; the\; QD \\ xm^*_{i,InN}(T)+(1-x)xm^*_{i,GaN}(T)\; elsewhere\; of\; the\; matrix \end{cases}$$
$$i(e,h) \quad (2)$$

The temperature dependence of the effective mass is given by [25]:

$$m_i^*(T)=\frac{m_i^*}{1+(C_i/E_g^i(T))} \quad (3)$$

where $m_i^*$ is the effective mass of the particle $i=(e,h)$ at room temperature, $E_g^i(T)$ is the band gap of a function of temperature, and $C_i$ is constant for each material. $C_i$ is equal to 14.07 *eV* for GaN, and to 25.50 *eV* for InN [24].

In Eq.(1), we describe the more realistic form of the confinement potential of particle i [24]:

$$V_i(r)=\begin{cases} \dfrac{Q_i\Delta E_g(x,T)r_i^2}{R^2}\; r_i\le R\; in\; the\; QD \\ \Delta E_g(x,T)\; elsewhere\; in\; the\; matrix \end{cases} \quad (4)$$

where $Q_e=0.70$ and $Q_h=0.3$ are the offset of the conduction band (valence band). $\Delta E_g(x,T)$ is the difference between the band gap of *InN* and *InGaN* which can be governed by the concentration of In and the temperature. It is expressed as:

$$\Delta E_g(x,T)=E_g^{In_xGa_{1-x}N}(x,T)-E_g^{InN}(T) \quad (5)$$

The bandgap energy of the ternary alloy $In_xGa_{1-x}N$ is given as follows [26]:

$$E_g^{In_xGa_{1-x}N}(x,T)=xE_g^{InN}(T)+(1-x)E_g^{GaN}(T)-bx(1-x) \quad (6)$$

where $b=1.43$ is the band gap bowing parameter.

**Table 1**
The forbidden band energy and the Varshni parameters (α and β) of *GaN* and *InN* materials.

| Parameter | *GaN* | *InN* |
|---|---|---|
| $E_g(eV)$ | 3.4 | 0.71 |
| $\alpha(meVK^{-1})$ | 0.593 | 0.245 |
| $\beta(K)$ | 600 | 625 |

While the forbidden energy gap generally depends on several physical factors such as temperature, it is necessary to mention its evolution as a function of temperature, which can be expressed by the Varshini formula [26]:

$$E_g(T) = E_g(0) - \frac{\alpha T^2}{T+\beta} \quad (7)$$

where α and β are the coefficients of temperature given in Table 1.

We use the finite difference method to solve the Schrödinger equation in order to calculate the energy levels in the QD *InN/InGaN* (for more details on the used method to solve the Schrödinger equation in the present paper, see ref [23]).

To illustrate the impact ionization effect on the *p-n* and *p-i-n* junction solar cell, we assume that the high energy of the incident photons of sunlight is given by $E > \theta E_g$ for $\theta > 2$ where $\theta$ is a parameter that depends on the type of the selected material. In the approximation of the effective mass, the value of $\theta$ is given by the following equation [14]:

$$\theta = 1 + \frac{2m_e^* + m_h^*}{m_e^* + m_h^*}. \quad (8)$$

Using the Eq. (2) of the effective mass of charge carriers in Eq. (8), expression of the parameter $\theta$ is given by:

$$\theta(T,x) = 1 + \frac{2m_e^*(T,x) + m_h^*(T,x)}{m_e^*(T,x) + m_h^*(T,x)}. \quad (9)$$

The average number of photons' occupancy provided by a thermal source can be expressed as [14]:

$$f(y) = (\exp(y) - 1)^{-1} \quad (10)$$

where $y = \frac{E}{kT_S}$ with $k$ is the Boltzmann constant and $T_S = 6000K$ is the thermal source. The flux of the incident photons from the sunlight is given by [14]:

$$g(y)d(y) = \left[\frac{2\pi(kT_s)^3}{h^3c^2}\right] y^2 d(y) \quad (11)$$

where $k$, $h$ and $c$ are the constant of Boltzmann, Plank constant and the speed of light in vacuum, respectively.

Taking into account the effect of impact ionization in a *p-n* junction, the thermodynamic efficiency Shokley-Queisser (S-Q) can be written as [14]:

$$\eta = \left(\frac{y_g}{D}\right)\left\{\int_{y_g}^{+\infty} f(y)g(y)dy + P\int_{\theta y_g}^{+\infty} f(y)g(y)dy\right\} \quad (12)$$

where $P$ is the average probability of the impact ionization occurs, i.e. probability that a charge carrier is generated following an impact ionization, and $D$ represents the energy flow in the case of a maximum concentration of the sun on the material. Note that $D$ is defined by Ref. 18:

$$D = \int_0^{\infty} yf(y)g(y)dy. \quad (13)$$

Its normal value is given by:

$$D = \frac{(2\pi)^5 E^3}{15h^3c^2y^3}. \quad (14)$$

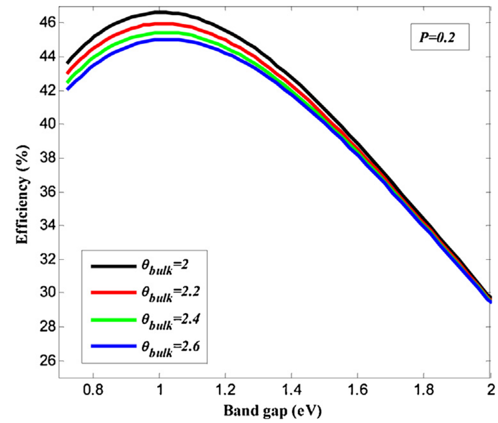


**Fig. 3.** Efficiency as a function of the band gap energy for different values of parameter of the selected material $\theta_{bulk}$.

The thermodynamic efficiency of the IBSCs is determined from the following expression [18]:

$$\eta = \left(\frac{y_g}{D}\right)\left\{\int_{y_g}^{+\infty} f(y)g(y)dy + P\int_{\theta y_g}^{+\infty} f(y)g(y)d(y) + \int_{y_h}^{y_g} f(y)g(y)d(y) + \int_{y_l}^{y_h} f(y)g(y)d(y) + P\int_{\theta y_l}^{y_g} f(y)g(y)d(y)\right\} \quad (15)$$

where $y_g = \frac{E_g}{kT_S}$, $y_h = \frac{E_H}{kT_S}$ and $y_l = \frac{E_L}{kT_S}$ are defined.

## 3. Results and discussion

In this section, after providing a brief description of the theoretical model for calculating the effects of impact ionization on the performance of the single-junction solar cell and the QD-IBSC solar cell based on QDs, we present and interpret the different obtained results. Then, we study the effects of temperature and indium concentration on the energy conversion efficiency of solar cells such as *p(InGaN)-n(InGaN)* and *p-(InGaN)-i(InN)-n(InGaN)* junction. In our calculations, we have assumed that cell thickness is large enough that all photons below the absorption threshold are absorbed, the IB is half filled with electrons, and the concentration of light solar is maximal.

First, we study the efficiency of *p-n* junction solar cells and show their variations with the energy band gap and the parameter $\theta$ of the selected material in the presence of the impact ionization process. In Fig. 3, we show the efficiency of the *p-n* junction versus the bandgap for different selected material parameter value $\theta_{bulk}$. In this figure, it can be seen that the efficiency is slightly decreased by increasing the values of the parameter $\theta_{bulk}$. A larger $\theta_{bulk}$ represents a larger effective mass of the charge carriers, a decrease in transition numbers in the efficient materials, and a decrease in the number of ionization transitions per impact. As a result, larger values of $\theta_{bulk}$ are equal to lower values of $P$ and reduced efficiency of the cell [27]. These results show that higher efficiency can be obtained by using the best materials that have an appropriate electronic mass and an effective mass.

In fact, larger $\theta_{bulk}$ represents the large masses of load carriers that are related to inappropriate hardware for SC and IBSC applications. For large effective mass values, the capacity of transporters for passage and transfer is reduced and causes non-radiative recombination and reduced efficiency [28]. Since the material type parameter strongly depends on the effective mass of the charge

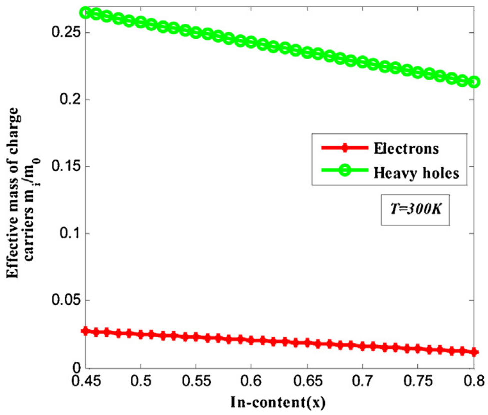


**Fig. 4.** Variation of the effective mass of electrons and heavy holes as a function of *In* concentration.

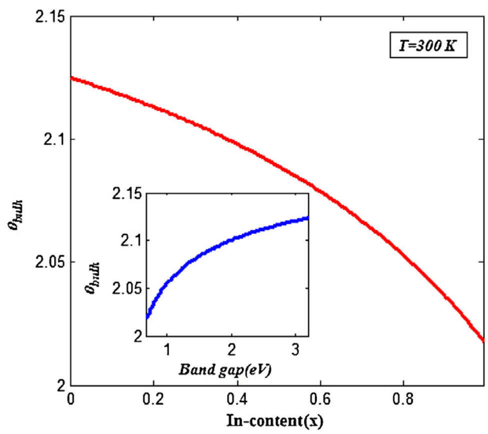


**Fig. 5.** The parameter $\theta_{bulk}(InGaN)$ of material type as a function of the *In* composition for *T* = *300* K.

carriers, we have shown in Fig. 4 the variation of the effective mass of electrons and heavy holes with the indium composition. From the figure we can see that the increase of the indium composition causes a significant reduction in the effective mass of charge carriers. At the same time, this sharp decrease in the effective mass of electrons and the heavy holes increases the electron mobility. However, it is important to take into account this variation in the calculation of energy conversion efficiencies of *p-n* and *p-i-n* junction solar cells.

In Fig. 5, we represent the variation of the parameter $\theta$ of bulk material as a function of the composition of *In* and as a function of energy gap of *InGaN* for a temperature in the order of *300* K. On the one hand, this figure shows that for a fixed temperature at *T* = *300* K, the parameter $\theta_{bulk}(InGaN)$ of bulk material declines with the concentration of *In*. This is due to the reduction of effective electron masses and holes with the *In* concentration (see Fig. 4). On the other hand, the $\theta_{bulk}(InGaN)$ parameter increases with the increase in *InGaN* gap energy. Indeed, the large values of the parameter $\theta_{bulk}(InGaN)$ correspond to the large effective masses of charge carriers with the energy gap of *InGaN*. They produce a decrease in the number of impact ionization transition and reduce efficiency. From the figure we note that $\theta_{bulk}(InGaN)$ strongly depends on the gap of the material and the doping concentration.

Figure 6 shows the evolution of the parameter $\theta_{bulk}(InGaN)$ with the temperature for an indium concentration of the order of 40%. The numbers clearly show that the temperature has only a minor effect on the ionization impact parameter of *InGaN* material. From Figs. 5 and 6 we noted that the parameter $\theta_{bulk}(InGaN)$ is affected by the composition of *In* and the temperature. Therefore, such properties contribute to an overall improvement in efficiency by tuning the optimized parameter $\theta_{bulk}(InGaN)$ of the selected material and improving the number of photons absorbed by the impact ionization process.

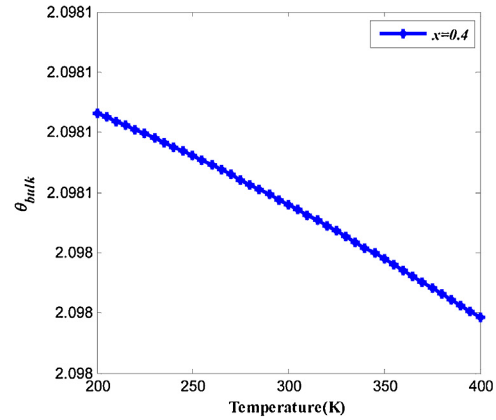


**Fig. 6.** The parameter $\theta_{bulk}(InGaN)$ of material type as a function of the *In* composition for T = 300 K.

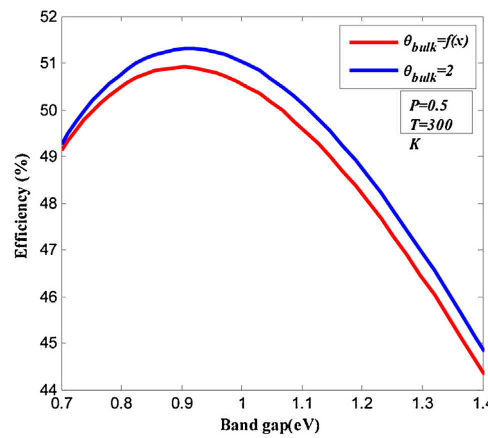


**Fig. 7.** Efficiency as a function of the forbidden band of energy for a fixed value of parameter of the selected material $\theta_{bulk}(InGaN)$ when one takes into account the variation of $\theta_{bulk}(InGaN)$ with the concentration of *In*.

We have shown in Fig. 7 the energy conversion efficiency of a single *p-n* junction solar cell based on *InGaN* material versus $E_g$ for a fixed temperature *T* = *300* K. In particular, the conversion efficiency are presented for two cases: (i) in the first case we fixed the parameter of selection of the material $\theta_{bulk}(InGaN)$, (ii) in the second case we took into account the variation of parameter of selection of the material when the composition of *In* and *InGaN* gap varies. We noted that the conversion efficiency is more affected when taking into account the effect of the composition of *In* on the parameter $\theta_{bulk}(InGaN)$. It would be interesting to take into account the effect of the indium content on $\theta_{bulk}(InGaN)$ in order to get an idea of the maximum efficiency of solar cells in presence of the ionization impact process.

On the other hand, Figure 8 gives the variation of the energy conversion efficiency for a *p(InGaN)-n(InGaN)* junction as a function of *Eg* for the probability of impact ionization *P* = *0.5* and for different temperature *T*=*(200,300,400* K*)*. As it can be easily seen, the energy conversion efficiency is reduced with the host temperatures. Then, the temperature variation affects these parameters and consequently, the performance of the solar cells. The reason for this is that photo-generated transporters with lower energy materials have a higher probability of recombination when the temperature becomes higher [29]. Several studies have pointed out that the

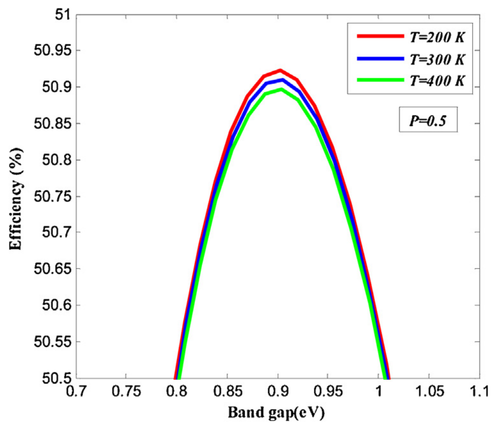


**Fig. 8.** The efficiency of *p-n* junction as a function of the bandgap energy for three different values of temperature *T= (200,300,400 K)*.

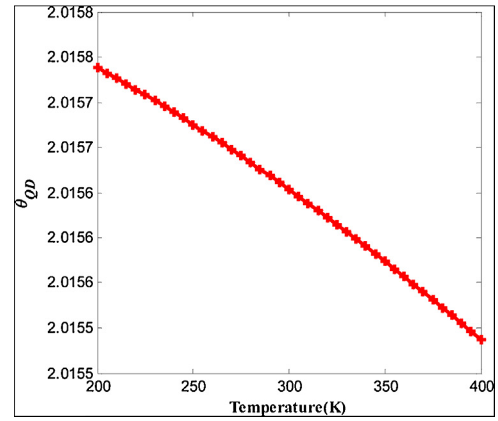


**Fig. 10.** The parameter $\theta_{QD}(InN)$ of material type as a function of *In* concentration for *T = 300 K*.

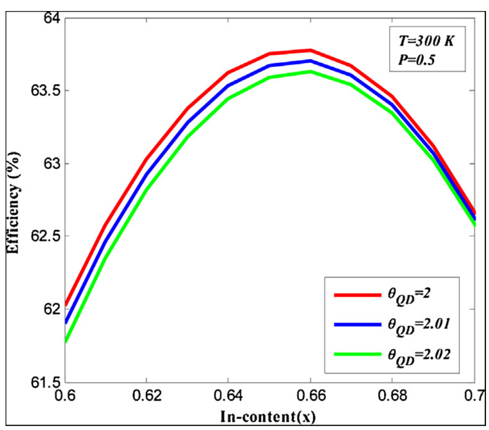


**Fig. 9.** Efficiency of a QD-IBSC as a function of *In* composition for three different parameter values of the selected material of QD $\theta_{QD}$.

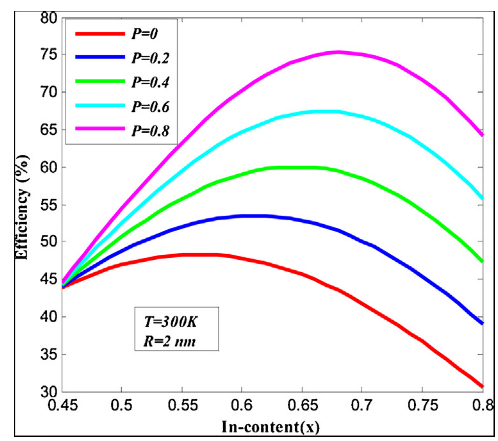


**Fig. 11.** Efficiency versus *In* content for six different values of the ionization impact probability *P*.

performance of solar cells reduced with increasing temperature [30,31].

In Fig. 9 we present the variation of the *QD-InN / InGaN* QD-IBSC efficiency as a function of the indium composition for different values of the QD material type parameter $\theta_{QD}$ and with a probability *P = 0.5* of the impact ionization. It is clear that the efficiency decreases when the parameter $\theta_{QD}$ increases. This is due to the large effective masses of the charge carriers. In addition, it is clearly demonstrated that the variation of $\theta_{QD}$ has an influence on the performance of the QD-IBSC. This representation clearly demonstrates the parameter type effect of the material chosen for QD. For further improvements in photovoltaic performance enhanced by the impact ionization process, a deeper understanding of the physical parameters on impact ionization processes is needed. For this purpose, we are interested in taking into consideration the effect of temperature and degree of substitution on energy conversion efficiency for QD-IBSC in the presence of the impact ionization process.

To study the impact of indium composition and temperature on the performance of *InN*-based QD-IBSC intermediate-band solar cells as a QD and *InGaN* as a barrier, first of all, we determine the effect of these parameters on the evolution of the material selection parameter for the *InN* QDs. In Fig. 10, we show the variation of the parameter of material type for the QD $\theta_{QD}(InN)$ as a function of temperature. As it can be seen in this figure, the $\theta_{QD}\,(InN)$ decreases with increasing temperature. Indeed, we observe that the temperature has a minor effect on the parameter $\theta_{QD}(InN)$.

We analyze the effect of indium concentration on conversion efficiency for *p-(InGaN)-i(QD-InN)-n(InGaN)* junction solar cells in the presence of impact ionization processes. For this purpose, we plot in Fig. 11 the efficiency against the content of indium for *T = 300 K* and a quantum dot radius of the order of *R = 2 nm* and for different values of impact probability ionization *P*. We observe that the conversion efficiency is improved by increasing the probability of ionization by impact. As it can be seen, without the impact ionization process *(P = 0)*, there will be a yield of approximately $\eta = 48.3\%$. In the presence of the impact ionization effect *(P = 1)*, the energy conversion efficiency reaches a maximum value of $\eta = 75.3\%$ using Eq. 15. Thus, it is clear that the influence of impact ionization process on efficiency becomes more important for the lower gap energies. We also observed a maximum offset of the parabola with the increasing probability of ionization by impact. Indeed, this is due to the low parameter values $\theta_{bulk}(InGaN)$ obtained for the large concentrations of *In*. In addition, by reducing the bandgap using more indium concentration, more photons were absorbed by *InGaN*, which led to an increase of $\eta$.

The schematic representation of the efficiency of an intermediate band solar cell *p (InGaN)-i(QD-InN)-n (InGaN)* are presented for *R = 2 nm*, for three values of the temperature *T = (200, 300, 400 K)* and for a probability of impact ionization *P = 0.5*. The purpose of this figure is to understand the effect of temperature on the conversion efficiency shown in Fig. 12. In the presence of impact ionization processes, the efficiency of the conversion of Q-IBSC solar cell *p (InGaN)-i(QD-InN)-n (InGaN)* decreases with increasing temperature. This is believed to be due to the low QD energy barrier and recombination effects in QD-IBSCs. It can also be concluded that

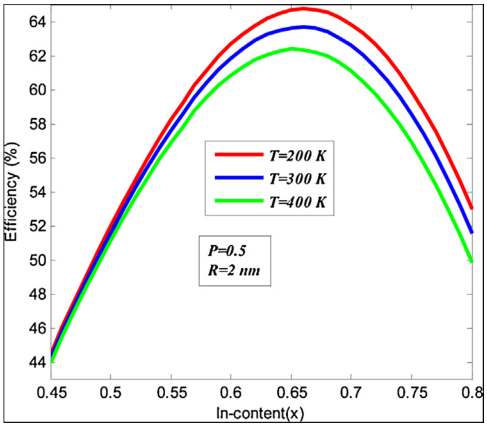


**Fig. 12.** Efficiency as a function of the *In* content for three different values of temperature.

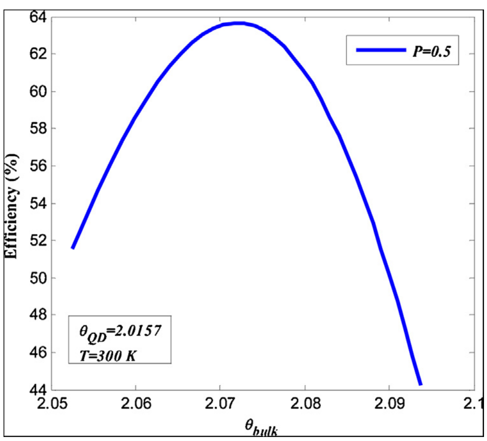


**Fig. 13.** Efficiency as a function of type material parameter of barrier.

the effects of low temperatures can improve the efficiency of the cell.

In the last part, we consider the impact ionization process *P* = *0.5*. Figure 13 shows the variation of the efficiency of an *InN/InGaN* intermediate band solar cell as a function of material type parameter of barrier $\theta_{bulk}(InGaN)$ for *R* = *2 nm*, *T* = *300 K* and $\theta_{QD} = 2.0157$. In fact, we varied the indium composition while η and $\theta_{bulk}$ vary with the latter and we traced the pace of $\eta$ as a function of $\theta_{bulk}$ to determine the optimal parameter for maximum efficiency. For *P* = *0.5*, we obtained a maximum efficiency of about 63.63% for the following optimal physical parameter: *x* = *0.65, T* = *300 K, R* = *2 nm* and $\theta_{bulk}(InGaN) = 2.073$.

## 4. Conclusions

In this work, impact ionization processes, energy conversion efficiency of conventional solar cells $(p(In_xGa_{1-x}N)\text{-}n(In_xGa_{1-x}N))$ and efficiency of QDs-IBSC intermediate band $(p(In_xGa_{1-x}N)\text{-}i(QDs\text{-}InN)\text{-}n(In_xGa_{1-x}N))$ solar cells were investigated. The calculation was discussed in the context of the effective mass approximation. In this paper, importance of perturbations such as indium composition and temperature, effect of *In* content and temperature on the impact ionization process coefficient of the selected material $\theta$ for the bulk *InGaN* substrate and *InN* quantum dot, energy conversion efficiency of solar cells *p-n* and *p-i-n* were studied. Taking into account the impact ionization process, the conversion efficiency of the *p-n* and *p-i-n* junction will be investigated. Our results demonstrated that the energy conversion efficiency of *InGaN*-based solar cells is strongly affected by indium concentration and poorly affected by temperature. In addition, the simulations show that temperature and high concentration of indium lead to a reduction of parameter of the selected material type. Furthermore, the latter performs a significant improvement in the energy conversion efficiency. Moreover, our calculations demonstrate that, in the presence of an impact ionization process, the efficiency of *p-n* and *p-i-n* junction solar cells is effectively improved for high doping concentrations of the *In* and low temperatures. These results show that *InGaN* proves to be a promising candidate for the realization of *p-n* and *p-i-n* junction solar cells.

## References

[1] V. Mlinar, Engineered nanomaterials for solar energy conversion, Nanotechnology 24 (2013), 042001, http://dx.doi.org/10.1088/0957-4484/24/4/042001.
[2] M.A. Green, S.P. Bremner, Energy conversion approaches and materials for high-efficiency photovoltaics, Nat. Mater. 16 (2017) 23, http://dx.doi.org/10.1038/nmat4676.
[3] A. Eddiai, M. Meddad, S. Touhtouh, A. Hajjaji, Y. Boughaleb, D. Guyomar, S. Belkhiat, B. Sahraoui, Mechanical characterization of an electrostrictive polymer for actuation and energy harvesting, J. Appl. Phys. 111 (2012), 124115, http://dx.doi.org/10.1063/1.4729532.
[4] A.K. Arof, H.K. Jun, L.N. Sim, M.Z. Kufian, B. Sahraoui, Gel polymer electrolyte based on LiBOB and PAN for the application in dye-sensitized solar cells, Opt. Mater. 36 (2013) 35–139, http://dx.doi.org/10.1016/j.optmat.2013.04.027.
[5] A. Luque, A. Marti, The intermediate band solar cell: progress toward the realization of an attractive concept, Adv. Mater. 22 (2010) 160–174, http://dx.doi.org/10.1002/adma.200902388.
[6] A. Luque, A. Martí, Increasing the efficiency of ideal solar cells by photon induced transitions at intermediate levels, Phys. Rev. Lett. 78 (1997), 5014, http://dx.doi.org/10.1103/PhysRevLett.78.5014.
[7] W. Shockley, H.J. Queisser, Detailed balance limit of efficiency of p-n junction solar cells, J. Appl. Phys. 32 (1961) 510–519, http://dx.doi.org/10.1063/1.1736034.
[8] M.C. Beard, A.G. Midgett, M.C. Hanna, J.M. Luther, B.K. Hughes, A.J. Nozik, Comparing multiple exciton generation in quantum dots to impact ionization in bulk semiconductors: implications for enhancement of solar energy conversion, Nano Lett. 10 (2010) 3019–3027, http://dx.doi.org/10.1021/nl101490z.
[9] O.E. Semonin, J.M. Luther, S. Choi, H.Y. Chen, J. Gao, A.J. Nozik, M.C. Beard, Peak external photocurrent quantum efficiency exceeding 100% via MEG in a quantum dot solar cell, Science 334 (2011) 1530–1533, http://dx.doi.org/10.1126/science.1209845.
[10] S.M. Hubbard, C.D. Cress, C.G. Bailey, R.P. Raffaelle, S.G. Bailey, D.M. Wilt, Effect of strain compensation on quantum dot enhanced GaAs solar cells, Appl. Phys. Lett. 92 (2008), 123512, http://dx.doi.org/10.1063/1.2903699.
[11] T. Sugaya, Y. Kamikawa, S. Furue, T. Amano, M. Mori, S. Niki, Multi-stacked quantum dot solar cells fabricated by intermittent deposition of InGaAs, Sol. Energy Mater. Sol. Cells 95 (2011) 163–166, http://dx.doi.org/10.1016/j.solmat.2010.04.040.
[12] A. Martí, N. Lopez, E. Antolin, E. Canovas, A. Luque, C.R. Stanley, C.D. Farmer, P. Diaz, Emitter degradation in quantum dot intermediate band solar cells, Appl. Phys. Lett. 90 (2007), 23351, http://dx.doi.org/10.1063/1.2747195.
[13] G. Jolley, H.F. Lu, L. Fu, H.H. Tan, C. Jagadish, Electron-hole recombination properties of in $_{0.5}$ Ga $_{0.5}$ As/GaAs quantum dot solar cells and the influence on the open circuit voltage, Appl. Phys. Lett. 97 (2010), 123505, http://dx.doi.org/10.1063/1.3492836.
[14] P.T. Landsberg, H. Nussbaumer, G. Willeke, Band-band impact ionization and solar cell efficiency, J. Appl. Phys. 74 (1993) 1451–1452, http://dx.doi.org/10.1063/1.354886.
[15] A. Luque, A. Martí, L. Cuadra, Impact-ionization-assisted intermediate band solar cell, IEEE Trans. Electron Devices 50 (2003) 447–454, http://dx.doi.org/10.1109/TED.2003.809024.
[16] S. Kolodinski, J.H. Werner, T. Wittchen, H.J. Queisser, Quantum efficiencies exceeding unity due to impact ionization in silicon solar cells, Appl. Phys. Lett. 63 (1993) 2405–2407, http://dx.doi.org/10.1063/1.110489.
[17] H. Movla, Influence of the inverse Auger process on the performance of InxGa1 – xN/GaN quantum dot solar cells, Opt. – Int. J. Light Electron. Opt. 127 (2016) 4799–4802, http://dx.doi.org/10.1016/j.ijleo.2016.01.156.
[18] N.E. Gorji, Impact ionization effects on the efficiency of the intermediate band solar cells, Physica E Low. Dimens. Syst. Nanostruct. 44 (2012) 1608–1611, http://dx.doi.org/10.1016/j.physe.2012.04.004.
[19] S.W. Feng, C.M. Lai, C.H. Chen, W.C. Sun, L.W. Tu, Theoretical simulations of the effects of the indium content, thickness, and defect density of the i-layer on the performance of p-i-n InGaN single homojunction solar cells, J. Appl. Phys. 108 (2009), 17350, http://dx.doi.org/10.1063/1.3484040.
[20] X.M. Cai, S.W. Zeng, B.P. Zhang, Fabrication and characterization of InGaN pin homojunction solar cell, Appl. Phys. Lett. 95 (2009), 173504, http://dx.doi.org/10.1063/1.3254215.

[21] A. Asgari, K. Khalili, Temperature dependence of InGaN/GaN multiple quantum well based high efficiency solar cell, Sol. Energy Mater. Sol. Cells 95 (2011) 3124–3129, http://dx.doi.org/10.1016/j.solmat.2011.07.001.
[22] H. El Ghazi, A. Jorio, Electron-hole transition in spherical QD-QW nanoparticles based on GaN|(In, Ga) N| GaN under hydrostatic pressure, Physica B Condens. Matter 15 (2013) 42–45, http://dx.doi.org/10.1016/j.physb.2013.07.025.
[23] N. Ben Afkir, E. Feddi, F. Dujardin, M. Zazoui, J. Meziane, Photovoltaic conversion efficiency of InN/$In_xGa_{1-x}N$ quantum dot intermediate band solar cells, Physica B Condens. Matter 1 (2018) 10–16, http://dx.doi.org/10.1016/j.physb.2018.01.005.
[24] H. El Ghazi, A. Jorio, Temperature dependence of interband recombination energy in symmetric (In, Ga) N spherical quantum dot-quantum well, Physica B Condens. Matter 1 (2014) 64–66, http://dx.doi.org/10.1016/j.physb.2013.09.017.
[25] Y.U. Peter, M. Cardona, Fundamentals of Semiconductors: Physics And Materials Properties, Springer Science & Business Media, 2010, April 7.
[26] Y.P. Varshni, Temperature dependence of the energy gap in semiconductors, physica. 34 (1967) 149–154, http://dx.doi.org/10.1016/0031-8914(67)90062-6.
[27] A. Luque, A. Martı, C. Stanley, N. López, L. Cuadra, D. Zhou, J.L. Pearson, A. McKee, General equivalent circuit for intermediate band devices: potentials, currents and electroluminescence, J. Appl. Phys. 96 (2004) 903–909, http://dx.doi.org/10.1063/1.1760836.
[28] A. Luque, A. Martí, L. Cuadra, Thermodynamic consistency of sub-bandgap absorbing solar cell proposals, IEEE Trans. Electron Devices 48 (2001) 2118–2124, http://dx.doi.org/10.1109/16.944204.
[29] J.J. Wysocki, P. Rappaport, Effect of temperature on photovoltaic solar energy conversion, J. Appl. Phys. 31 (1960) 571–578, http://dx.doi.org/10.1063/1.1735630.
[30] J.C. Fan, Theoretical temperature dependence of solar cell parameters, Sol. Cells 17 (1986) 309–315, http://dx.doi.org/10.1016/0379-6787(86)90020-7.
[31] P. Singh, S.N. Singh, M. Lal, M. Husain, Temperature dependence of I–V characteristics and performance parameters of silicon solar cell, Sol. Energy Mater. Sol. Cells 92 (2008) 1611–1616, http://dx.doi.org/10.1016/j.solmat.2008.07.010.